RESEARCH PAPER

Analysis of interfacial mixing zone and mixing index in microfluidic channels
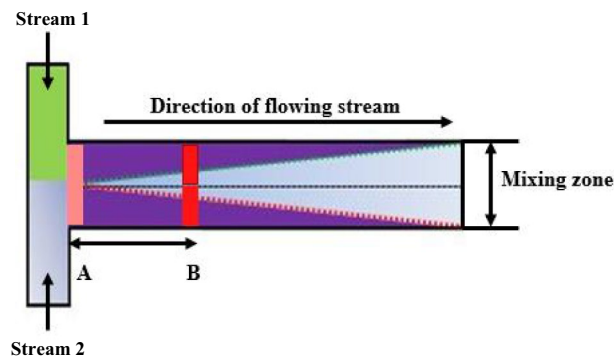
Paritosh Agnihotri[1] ®

Abstract

Maintaining the interfacial mixing zone is very important for many micro-engineering and nano-technological applications. Many applications including controlled separation of nanoparticles in microfluidic devices, chemical reactions, mechanical separations, cell sorting and various biomedical applications require desired width of the interfacial mixing zone. Co-laminar flow and the flow rate of the liquid streams have been found to influence the interfacial mixing zone in the microfluidic flow. Passive microdevices utilise no energy inputs except the pressure head used to drive the flow at constant flow rates. In considering such situations, the flow has a laminar flow pattern, and hence mixing relies due to the convection–diffusion effect to separate and increase the contact time between flowing streams. In this paper, the behaviour of fluid mixing is demonstrated in T-shaped microdevices (micromixers) with a rectangular cross-sectional at low Reynolds numbers. Three water-soluble dyes and deionised water having almost the same densities and viscosities were used to characterize the interfacial mixing zones which formed at the centre of the microchannel. Results showed that interfacial mixing is related to diffusivities of flowing streams, flow rates and geometries of microchannels. Mixing performance and analytical evaluation of diffusive mixing are also reported in the paper. The present work provides a platform for the design of novel microfluidic devices to control diffusion processes for applications such as absorption, extraction, crystallization, capture of molecules or nanoparticles.

Graphical abstract

✉ Paritosh Agnihotri
  paritoshagni@gmail.com

1 Department of Chemical Engineering, Sardar Vallabhbhai
   National Institute of Technology, Ichchhanath, Surat,
   Gujarat 395007, India

1 Introduction

Molecular diffusion plays an important role in the mixing of co-laminar flow for microfluidic applications. Over the last few years, mixing in microfluidic devices has been a great subject for researchers working in the field of micro and nanoengineering for biological, biomedical and energy

applications. Many process applications including separation, chemical reaction, crystallization, etc. require a controlled interaction time to generate particles of the desired size, as well as to get the desired concentration of the outlet streams. This can be mostly controlled by maintaining the interface between the interacting streams at the desired location inside the microchannel. Maintaining the interfacial mixing zone is very crucial for mechanical separations, chemical reactions, cell sorting and various biomedical applications. Controlling the position of the interface in microchannels is having direct implications on the volumetric fractional holdup occupied by the streams in the microchannels. Accurate control of the residence time inside the microfluidic device is important for achieving the predictable progress of reaction or degree of separation. For instance, the synthesis of nanoparticles from a bottom-up approach using Lab-on-a-Chip techniques can be achieved by controlling the diffusion of the reactants inside the microchannels. Kim et al. (2017) have reported that the diffusion and mixing in microchannels as important factors affecting the size and polydispersity of nanoparticles synthesized using microfluidics. Miniature devices comprising the microchannels offer enhanced transfer processes (Bae et al. 2016; Cho et al. 2016) and chemical reactions (Reckamp et al. 2017). Controlled formation of microdroplets (Li and Barrow 2017; Sesen et al. 2017), crystals (Shi et al. 2017) and synthesizing the vesicles of desired shape (Mally et al. 2017) using microfluidics also need careful control of the hydrodynamics inside the microchannels. This requires control over the contacting interface inside the microchannels which ultimately governs the diffusion across the interface to affect the formation of dispersed phase with controlled hydrodynamics.

The basic studies of steady-state diffusion in T-shaped microchannel with rectangular geometry were evaluated by Kamholz et al. (1999, 2001), Ismagilov et al. (2000), and they showed that concentration distribution occurred by diffusive and convective transport within these microchannels. Kamholz et al. (1999) revealed that rectangular microchannel velocity profile will be parabolic across the narrow dimension, called width and mostly uniform at wider dimensions called diffusion dimension. Kamholz et al. (2001) defined the term "interdiffusion" as the critical dimension that governs the extent of interdiffusion in the diffusion dimension along which diffusion occurs between streams. The formation of the interdiffusion region is due to the difference in diffusion coefficients between two diffusive streams. Ismagilov et al. (2000) established the logical use of laminar flow for patterning and fabrication within microchannels needs an improved understanding of the convective-diffusive transport processes within the walls of the channel. The width of the reaction–diffusion zone at the interface just to the wall of the channel and

transverse to the direction of flow. The increase of transverse diffusive mixing can be decreased by increasing the average flow rate. Reynolds number should be maintained low so that the flow is laminar. The increase of transverse mixing near the centre of the channel at this point flow rate is nearly constant (Hatch et al. 2004) made use of molecular interactions based on the diffusive transport and studied molecular binding interactions using hydrogels for diffusion-based analysis. At microscale devices for low Reynolds number when two inlet streams display laminar flow behaviour. They mixed at the junction and flow side by side through the main channel with diffusion besides convection controlling the mixing of the two fluids. Tan and Neild (2012) studied microfluidic mixing in Y-shaped open channel. They found that open fluidic channels have ability to interact with the surrounding air environment that facilitates desired mixing.

Microfluidic systems can offer size-based interface properties to utilize a wide range of applications (Atencia and Beebe 2005). As the systems are reduced in size, a laminar flow pattern at a low Reynolds number is established. In this condition surface-dependent properties such as surface tension and viscosity can dominate over volume-dependent properties, providing new microscale phenomena to confine liquid–liquid interface in a microchannel with the co-laminar flow can be formed (Mousavi Shaegh et al. 2011). Kumar et al. (2011) and Hetsroni et al. (2005) discussed the single-phase fluid flow in smooth as well as rough microchannels. Experimentally it was shown that the friction characteristics of both microchannels are remarkably different. For various flow rates, the roughness enhances friction factor at the same Reynolds numbers. Microfluidic devices show some fundamental differences between the physical properties of fluids moving in macro-meter-scale channels and those flow through micrometre-scale channels. Squires and Quake (2005), Stone et al. (2004) and Janasek et al. (2006) differentiates macroscopic and microfluidic system that greatly relates to lab-on-a-chip devices and point out the very essential difference is turbulence. At low Reynolds number viscous effects dominates over inertial effects whereas surface forces are much more important than body forces. Atencia and Beebe (2005) reported different types of interfaces and their consequences for microfluidics which are useful for specific objectives of microfluidic mixing as briefly summarized in Table 1. Diffusion or convection, electromigration and chemical reaction are the different modes of mass transport within microfluidic devices. Generally, microfluidic flow is incorporated by high Peclet numbers (Choban et al. 2004) which depicts that the rate of transverse diffusion is much lower than the streamwise convective velocity, and the diffusive mixing is limited to a thin interfacial width at the centre of the channel and developed in increasing in size in

Table 1 Brief inference on the features of different types of microfluidic interfaces (Atencia and Beebe 2005)

Sr. No	Microfluidic interfaces	Characteristics of interfaces	Applications
1	Floating interfaces	Formed between immiscible fluids, To produce droplets of precise shape and varying content	Act as a permeable wall for performing and analysing reactions, Transporting cargo
2	Pinned interfaces	Formed between immiscible fluids, Maintained by the action of capillary forces and act as membranes	Drugs partitioning behaviour, Enzymatic reactions, Solvent extraction of metal ions, Phase transfer reactions (PCR)
3	Dynamic or moving interfaces	Formed between miscible fluids under laminar flow conditions, Creating a diffusive interface with certain geometry	Molecular mass sensors, Chemical assays, Membraneless microfluidic fluidic fuel cells, Immunoassays
4	Secondary interfaces	Formed between miscible fluids, Formed due to diffusion and creates a complex but certain interfaces of solute	Screening of protein crystallization

the downstream position. This interfacial width is sometimes known as the interdiffusion zone or interdiffusion width.

2 Mixing in microfluidic devices

Mixing in microfluidic devices is described by three dimensionless parameters, the Reynolds number (Re), Peclet number (Pe) and Strouhal number (St). The ratio of inertia force to viscous force (Re $= \frac{UL}{\vartheta}$) measures the nature of flow and quantifies the relative importance of forces. The Peclet number (Pe $= \frac{UL}{D} = \frac{T_{diff}}{T_{conv}}$), describes the ratio between diffusion and convection phenomena (Nguyen and Wu 2005). The Strouhal number (St $= \frac{fD}{U}$) which represent the active micromixer, defined as the ratio between the residence time of a species and the period of its disturbance. These numbers are associated with characterizing the mixing performance in microfluidic devices. Synthesis or crystallization of nanoparticles in single-phase continuous flow microfluidic devices are designed to work at low Re (< 10), the initial mixing mechanism is molecular interdiffusion through laminar streams in the absence of turbulence (Ma et al. 2017). The mixing time is associated with the microchannel width and flow rates of the streams (Johnson et al. 2002; Hessel et al. 2005). The small dimensions of a microchannel will promote a decrease in mixing time to even milliseconds which is beneficial for nano synthesis (at the nucleation stage). Aubin et al. (2010) explored that mixing which is based on molecular diffusion is a very slow process. Particularly slow mixing is desirable for liquids having small diffusivities. So that it is important to achieve effective mixing in a desirable time, fluids must be employed in such a way that the interfacial surface between the flowing fluids is increased tremendously and the diffusional path is reduced. In microfluidic devices (T- and Y- shaped microchannels) merges two liquid streams into a common single channel to generate a controlled diffusive interface. One stream

contains an analyte and the other a tracer compound mostly preferred a fluorescent dye once they meet the broadening of the interface started during the initial stage of diffusive mixing. An interesting and useful property of T-shaped microchannels is that the reagent initially interdiffusion and reacts until the two liquid streams are in contact, so that time available for diffusion and reaction correspondence with the distance as covered by moving liquid streams. An outsider will willing to see the course of reaction and diffusion as a still image and diffusion distances and reaction kinetics can be measured as a function of distance rather than time. The basic T-shaped microchannels are frequently for use in membraneless microfluidic fuel cells (Ferrigno et al. 2002; Choban et al. 2004), chemical assays (Kamholz et al. 1999) and immunoassays (Hatch et al. 2001).

The streams that enters from the two inlets of the channel are brought together into the main channel and flow downward, side-by-side and parallel to each other. If they are miscible, a diffusive interface forms with the help of the time scale of diffusion and convection, and the width of the diffusion zone can be measured. Ismagilov et al. (2000) showed that a chemical reaction between two reactants within a microchannel forms a fluorescent complex interface and, therefore, creates a visible diffusion zone.

Ottino and Wiggins (2004) discussed the importance of mixing length and time scales in microfluidics. They reported that flow in microfluidic devices is generally viscous dominated having a parabolic velocity profile. The molecular diffusion coefficient ranges between 10^{-5} cm^2 s^{-1} to (low molecule) 10^{-7} cm^2 s^{-1} (large molecule). So that the values of convective to diffusional time scales can be evaluated using the Peclet number (Pe $= \frac{UL}{D} = \frac{T_{diff}}{T_{conv}}$), and range between 10^1 and 10^5, showing that convection is much faster than molecular diffusion. Thus, molecular diffusion may not be dominant in homogenizing the system to molecular scales in a reasonable period. The diffusional time scales for diffusing half of the width of the channel

is equal to the ratio of height/depth of the channel and diffusion coefficient.

If two miscible fluid streams flowing side by side, the diffusional distance, covers the entire width of the channel after a distance that is equal to the velocity of the flowing stream and time for diffusion.

Here, we discussed the microscopic observation and measurement of liquid–liquid interfacial mixing zone within T-shaped microchannels with water-based highly soluble azo dyes namely; Acid red, Allura Red and Rhodamine 6G.

The two non-reacting streams, diluted dye (colourful region) and deionised water (colourless region) are brought in contact with each other at the junction to flow side by side underflow laminar conditions.

The mixing is characterized in terms of the width of the interdiffusion zone, or generally known by some other names like diffusive displacement, the extent of diffusion, diffusion broadening, and width of the region mixed by diffusion, pronounced by different authors (Ismagilov et al. 2000; Kamholz and Yager 2001). The width of the diffusion zone is a measure of the distance of diffusive mixing across the fluids interface with the concentration intensity.

3 Materials and methods

3.1 Preparation

The T-shaped microchannel with a rectangular cross-section is one of the most frequently used passive micromixers. It consists of two inlet channels and a mixing channel. Three different sizes of T-shaped microchannels were fabricated using soft lithography as reported by Xia and Whitesides (1998). Briefly, the molds were prepared using aluminium sheets. The geometry of the channels was created by placing the plastic strips of the desired dimensions. Polydimethylsiloxane (PDMS) Sylgard 184 and curing agent (Dow Corning, Midland, USA) are used for the fabrication of microchannels. Liquid PDMS (silicon elastomer base material) and curing agent were mixed in a 10:1 (mass/mass) ratio, poured onto the prepared molds after removing air bubbles. Afterward, the mold was heated in an oven at 65 °C for 45 min. The solid transparent PDMS slab was formed and peeled off from the mold. The inlets and outlet ports were punched with a blunt needle in the PDMS. Finally, the micopipptes were attached with PDMS and device is ready for experiments.

A fluorescent solution is prepared using deionized water (Millipore, ELIX 10, Bangalore, India). The three azo dyes highly soluble in deionized water were used to analyse the flow behaviour in the microchannels and named as sample 1(Water-Acid red), sample 2 (Water-Allura red) and sample 3 (Water-Rhodamine 6G) with the concentration of 100 μM.

All the dyes were purchased from Sigma-Aldrich, Banglore, India. All the dyes were completely dissolved in water using a stirrer and ultrasonic waves. The diffusion coefficient of Acid red, Allura Red and Rhodamine 6G in water are 5.01×10^{-13} to 1.30×10^{-12} m^2 s^{-1}, $3.6 \pm 0.4 \times 10^{-10}$ m^2. s^{-1} and 2.8×10^{-10} m^2. s^{-1}, respectively (Ansari et al. 2018).

Two single multi-channel syringe pumps (NE-4000, NE1600, New Era Pump System, NY, USA) were used to control the flow rate ranging from 100–110 μl min^{-1} and 100–99 μl min^{-1}. During the experiments, deionized water (colorless) and deionized water-dye (colourful) streams were pumped into microchannel through inlet-1 and inlet-2 as shown in Fig. 1.

3.2 Experimental setup

An inverted microscope (ECLIPSE TS-100, Nikon, Japan) connected with a halogen lamp recognize the visualization of flow with a magnification of 10. A high-resolution digital camera (DS-U3, Canon, Japan) is mounted on the microscope to record the images and computer-based imaging acquisition software (NIS-Element F4.00.00. Ink) was used to measure the width of the mixing zone. Mixing is observed and measured when the dye is homogenously mixed and stable across the channel cross-section. Ismagilov et al. (2000) used confocal fluorescent microscopy to observe the fluorescent product formed by reaction between chemical species in microchannels. In the case of a non-circular cross-section of the flow channels, the hydrodynamics length or characteristic length (l^*) for the rectangular cross-sectional area of the microchannel is measured by the given equation.

$$l^* = \frac{2xy}{x + y} \tag{1}$$

where x and y are the width and depth or height of the microchannel, respectively.
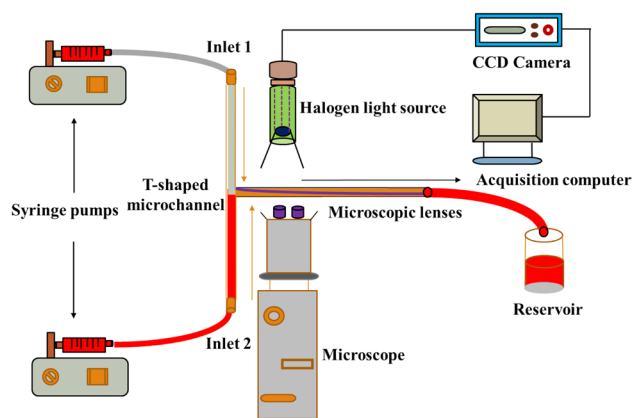

Fig. 1 Schematic representation of microfluidic set-up

We select the large relative length of microchannels for the experiments $<l/l^*$ where l is the length of microchannel and l^* is the characteristic length that is the diameter or depth of circular or rectangular microchannels, respectively.

The mixing phenomena of two co-flowing streams in pressure-driven microchannels having different aspect ratios (channel width/channel height = 0.68, 1.08, 1.16) were analysed over the wide range of flow rates. Pressure-driven microfluidic devices promote such flow which is typically parabolic-like profile across the liquid–liquid interface in a microchannel. Pressure-driven flow is commonly applied in microfluidic applications. The parabolic velocity profile creates a significant difference in the residence time of diffusive transport between the top, bottom walls and centre of the channel. The variation of diffusion concerning their position may largely affect the measurement intensity as well as molecular properties. The image of the mixing zone was acquired using an inverted microscope is connected with an image acquisition and processing system consisting of a CCD camera. The region of interest (ROI) of the CCD camera is fixed 512×512 during all experiments.

4 Results and discussion

4.1 Diffusive dominated mixing related to flow rates, Reynolds number and aspect ratios

Molecular diffusion and convective transport due to electromigration, chemical reaction, and pressure gradient are the different modes of mass transport within microfluidic devices. When the dimensionless number, Peclet number is very small $(P_e \ll 1)$ convection is very slow as compared to diffusion and the reagents transport occurred only due to diffusion. The single-phase conninuous flow microfluidics is very attractive that improves throughput by performing multiple reactions in parallel (Zhao et al. 2011), to synthesis a large amount of nanoparticles with great reproducibility.

The laminar nature of fluid flows arises at low-Re in the state of microfluidics, mixing occurred only due to diffusion, which can result in long mixing times of order minutes or more. Purely diffusive mixing is desirable or not it depends on applications. Laminar flow region ensures a well-controlled reaction but it has also proven to be a very efffective method to study the flow effect during the crystallization processes (Puigmartí-Luis 2014).

The two streams flowing through microfluidic rectors require rapid mixing, which allows the dynamics of the reactions to be considered, rather than the diffusive dynamics of the molecules. The reverse problem is occurred in sorting and analyzing the products of those same reactions—the faster the mixing, the separation becomes tougher.

Controlling dispersion in microfluidic devices is often of paramount importance.

The basic T-shaped microfluidic devices in which two fluids are injected to flow parallel side-by-side. The time required for the mixing to be homogenized within the mixing channel is based on the particles or molecules to diffuse across the entire channel and is easily calculated as follows $t_d \sim w^2/D$ where w is the width of the channel. During this time the diffusion zone (strip) will change its position and covered a distance which is given as $Z \sim V_0 w^2/D$ in the downward of the channel.

The width of the colour region in the mixing channel mainly depend upon the diffusion coefficient, the geometry of the channel, flow rates and physical properties of the streams such as density and viscosity (Gambhire et al. 2016). The transverse component of the flow is managed to improve the mixing quality can be formed in microchannels by continuously streaching and folding flowing streams. Herringbone microchannels (staggered shaped) have the ability to exponentially increase the interface (mixing zone) between two fluids to attain fast mixing (Marschewski et al. 2015).

Here is the demonstration of the collective spreading of aqueous dye streams (colour) into nearby deionized water (colourless) streams for increasing and decreasing flow rates in the downstream direction. The increasing flow rates varies from 100 to 110 µl min^{-1} and that of decreasing flow rates varies from 99 to 90 µl min^{-1}. The width of the mixing zone is starting to grow as both streams meet through the length scale of the channel. It was observed that the change in the width of the mixing zone at the centre of the channel is large for liquid system 3 as compared to the other two liquid systems i.e. 1 and 2 (from Fig. 2a) due to the high diffusivity of R6G in water. Previously it was also shown that the fluids near the top and bottom move very slowly than that of the middle because of the spreading of the colour stream near the top and bottom walls to relate with $z^{1/3}$ whereas the middle of the channel varies with $z^{1/2}$ (Ismagilov et al. 2000). Therefore, tracers do not have as far downstream as they diffuse across the flowing stream.

If the velocity of the flowing stream increases a very less time is available for diffusive mixing. Thus, the required mixing length will be decreased. Consequently, increasing flow velocity will reduce the mixing length. It was also confirmed that the stream in large depth microchannels requires less time to diffuse and reach towards the side walls. Therefore, the mixing length is smaller in deeper microchannels. By increasing stream velocity, diffusion will be very fast so that a shorter mixing length is required (Rismanian et al. 2019). deMello, worked on continuous crystallalization of particles using microfluidics and demonstrated that on increasing the volumetric flow rates significantly improved the monodispersivity of colloids particles (Demello 2006).
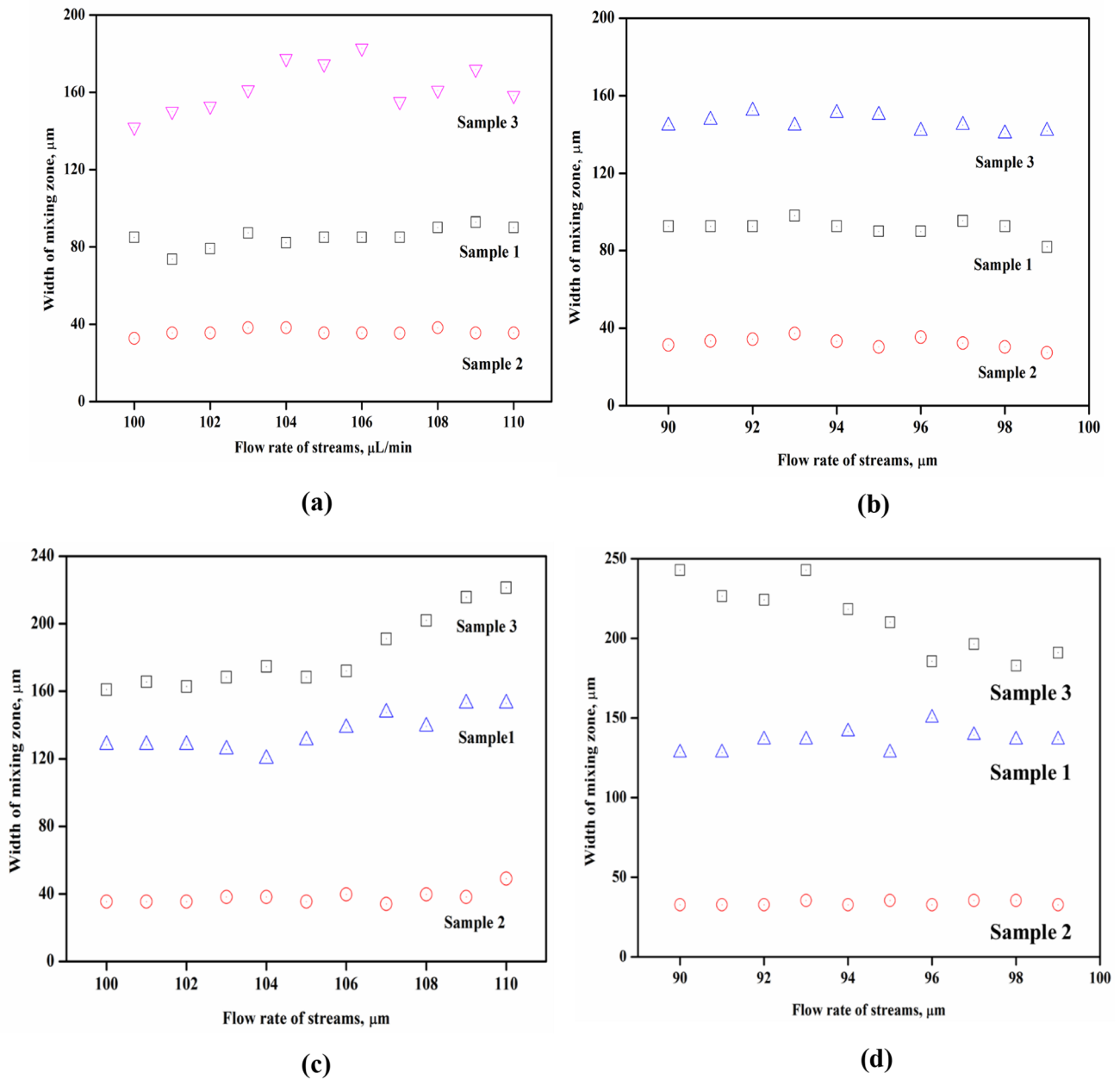
Fig. 2 Diffusion dominated mixing in T-shaped microchannel: For increasing and decreasing flow rates in a microchannel with aspect ratio 0.68 (**a**, **b**), for increasing and decreasing flow rates in a microchannel with aspect ratio 1.08 (**c**, **d**), for increasing and decreasing flow rates in a microchannel with aspect ratio 1.16 (**e**, **f**), mixing width variations at two distinct places in the direction of flowing streams. Sample 1 (**g**), sample 2 (**h**)

The spreading nature of dyes can be easily controlled by changing the flow rate of the streams It is displaced from the centre of the channel and vigorous mixing taking place in the downstream direction. It also shows that the spreading nature of R6G dye in deionized water is very large due to their high diffusion coefficient. For decreasing flow rates, the mixing width decreases as the flow rates were decreased for all three systems as shown in Fig. 2b.

At a low flow rate in the microchannels, the viscous forces dominate in the flow and any perturbation by irregularities and discontinuities in the mixing channel is damped out by the viscous forces. Therefore as predicted the nature of the flow is laminar (Wong et al. 2004). Control over the spreading of the width of the mixing zone for R6G is much more difficult as compared to the other two liquid streams because of its higher diffusivity.
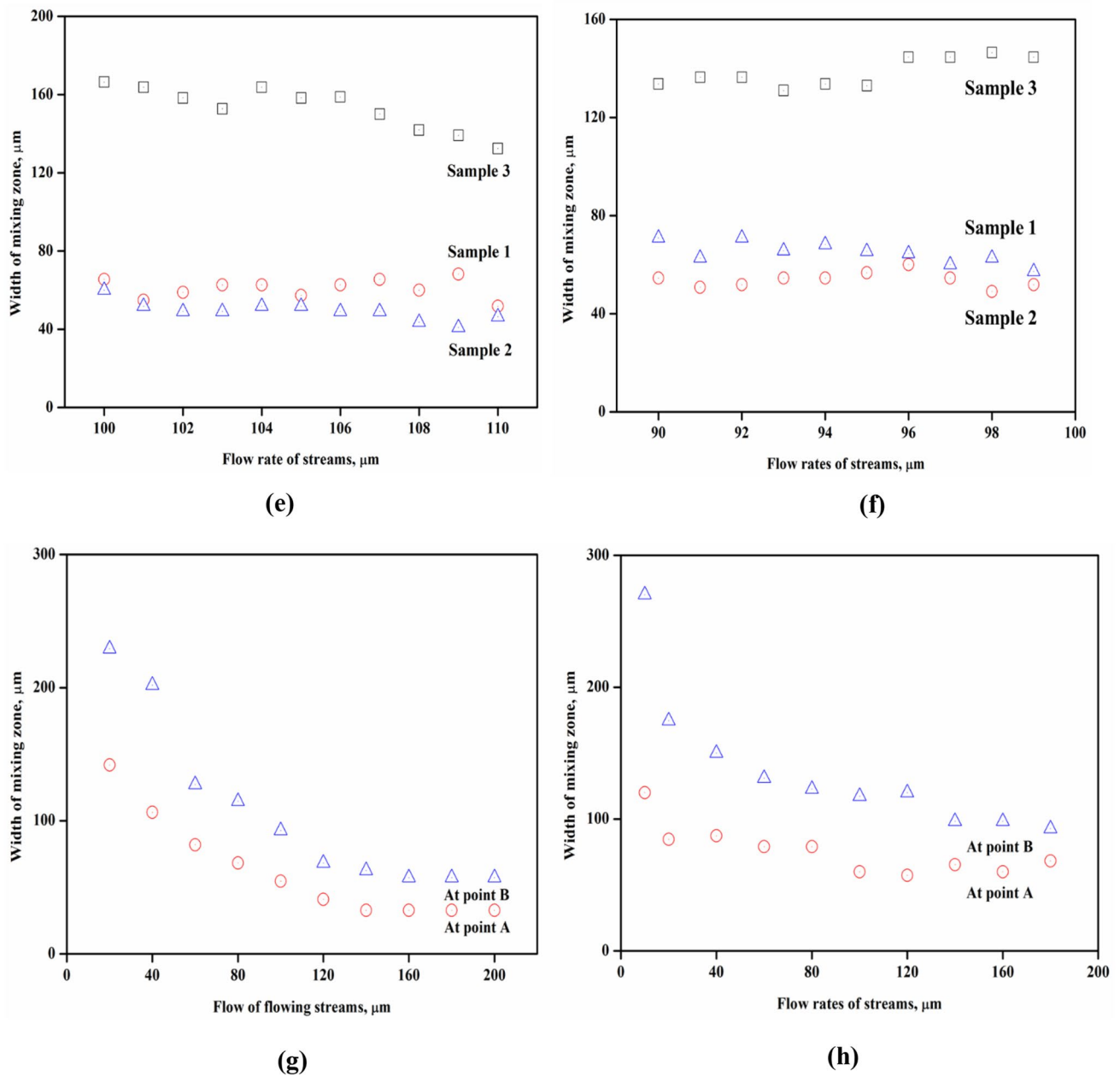
(e)

(f)

(g)

(h)

Fig. 2 (continued)

As the change in the aspect ratio of the microchannel (A.R. = 1.08), it was found that the spreading behaviour extended up to a large distance. For liquid system 1, mixing width increased sharply as compared to the other two liquid systems which showed that not only flow rate and diffusivity but a change in the flowing area of the mixing channel provide to control the mixing zone up to large extent. It supported that the spreading nature of acid red samples in deionized water is higher due to its large diffusivity. Under the same condition, the width of the mixing zone was measured for decreasing flow rates. In this situation, the available

contact time for diffusion increases and the width of the mixing zone grows at a large scale and it becomes difficult to control the mixing zone within the microchannels as shown in Fig. 2d.

Microchannel with A.R. = 1.16, the collective spreading of diffusive mixing zone for increasing flow rates once again higher for sample 1 and sample 2 we can say that by increasing the aspect ratio of the microchannels promotes to increase flow area for flowing streams consequently, the width of mixing zone and it's become difficult to the maintained displacement of mixing zone as shown in Fig. 2e.

Previously it was reported that displacement occurred in the interdiffusion mixing zone is due to coupling between hydrodynamics and mixing through the dependence of physical properties of streams that is density and viscosity (Dambrine et al. 2009). However, the width of the mixing zone was again found higher for liquid system 1 on the other hand remaining two systems showed low variations in the width of the mixing zone due to their lower diffusivity in water as shown in Fig. 2f.

We also express the measurement locations of the interdiffusion mixing width at the two distinct places within the microchannel and named as 'A' at the junction and 'B', 1002 µm distance from the junction in downward directions.

Under these conditions, the inlet flow streams were in the ratio of 1:2 varies from 10 to 180 µl min^{-1} for dye-containing liquid stream whereas flow rates of water stream vary between 20 and 200 µl min^{-1}.

From Fig. 3g it is observed that the width of the mixing zone decreases gradually as the flow rate of streams increases. For the liquid system, sample 2 the measured width of the mixing zone is at point B large as compare to junction A. It also shows that the collective spreading of the colour stream in a colourless stream decreases along
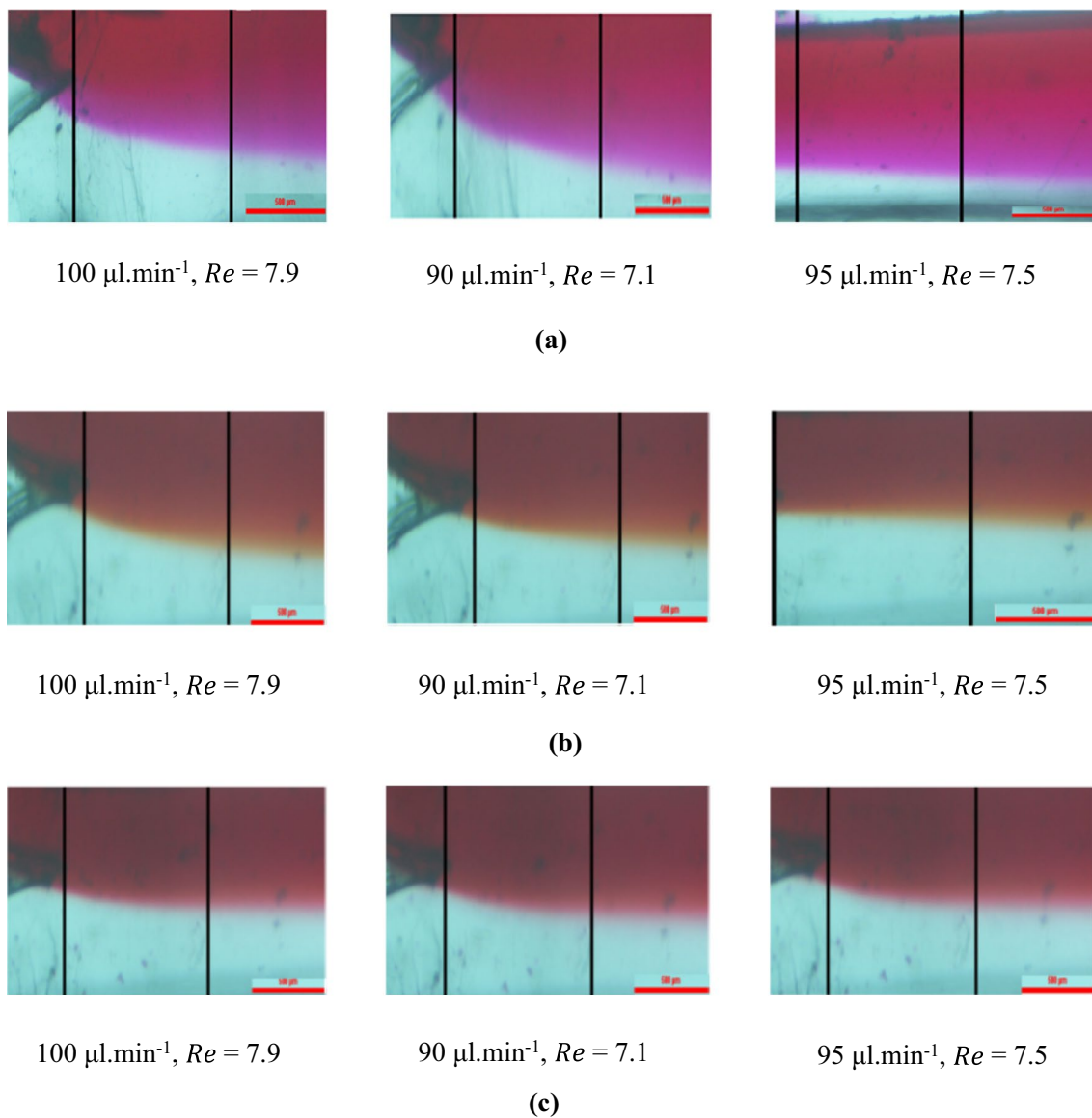

100 µl.min^{-1}, Re = 7.9   90 µl.min^{-1}, Re = 7.1   95 µl.min^{-1}, Re = 7.5

(a)

100 µl.min^{-1}, Re = 7.9   90 µl.min^{-1}, Re = 7.1   95 µl.min^{-1}, Re = 7.5

(b)

100 µl.min^{-1}, Re = 7.9   90 µl.min^{-1}, Re = 7.1   95 µl.min^{-1}, Re = 7.5

(c)

Fig. 3 Images for characterization of convective—diffusive dominated mixing in T-shaped microchannels at different Re. (**a**) Sample 1 (**b**) Sample 2 (**c**) Sample 3. (Scale bar: 500 µm)

the length of the microchannel. While increasing the flow rates decreases the mixing length of the flowing stream. Again, similar mixing behaviour is observed for sample 1 and sample 3 systems as shown in Figs. 3h. The mixing zone begins to grow from the junction of the channel and gradually decreases along the mixing length concerning the change in flow rate.

Figure 3 shows the experimental images of variations in the mixing zone along the length of the mixing channel for Re = 7.9, Re = 7.1 and Re = 7.5 as shown in Fig. 3a–c, respectively. Quality of mixing improved as the flow rate of streams increased and was better at the exit. However, it shows higher variations in the width of the mixing zone thus convective mixing outplays diffusive mixing.

The Reynolds number (Re) well known dimensionless number closely related to microfluidics. An important feature of microfluidics is the relatively slow mixing of fluids due to laminar flow at low Re.

(a)

(b)

Fig. 4 Variations in the mixing zone. (a) Increasing Reynolds No. (b) Decreasing Reynolds No

However, Wang et al. (2014) reported that turbulence can be created by an electrokinetically forced pressure-driven microfluidic flow in a channel with Re of order 1.

Figure 4a established the relationship between dynamic variation in the mixing zone with increasing Re. It was observed that for sample 3 created higher variations in the mixing zone as the higher diffusivity of R6G in water whereas in the other two systems the variations in the mixing zone are low because of slow diffusivities of dye streams. As Re increase s, the inertial forces become more apparent. Furthermore, the nonlinear inertial term destabilizes the flow as Re still increasing, resulting in unacceptable, irregularity in mixing zones. In a standard circular pipe where Reynolds number where the transition (laminar to turbulent) occurs for Re between 2000 and 3000. Such Re are significantly higher than those encountered in microfluidic devices, therefore microfluidic flows generally fall within the laminar flow regime. Our previous work showed that there is a significant increase in the mixing zone within the microchannel with an increase in Re. In addition, variations in the position of interdiffusion width were due to the coupling between hydrodynamics and mixing affected by the relative velocities of the fluid streams and the geometry of the microchannels (Agnihotri and Lad 2018). In addition, when Re is higher, increasing flow rates and decreasing the residence time consequently effect the process of molecular diffusion gradually.

The relationship between variations in the mixing zone for decreasing Re is reported in Fig. 4b. At very low Re where the flow is strictly laminar or stratified the entire mixing in the mixing channel is dominated by molecular diffusion within the mixing zone due to slow flow rate, long residence time, and more possibilities for radial mass transport (He et al. 2019). From the figure, less variation in the mixing zone is observed for sample 3 because of its higher diffusivity.
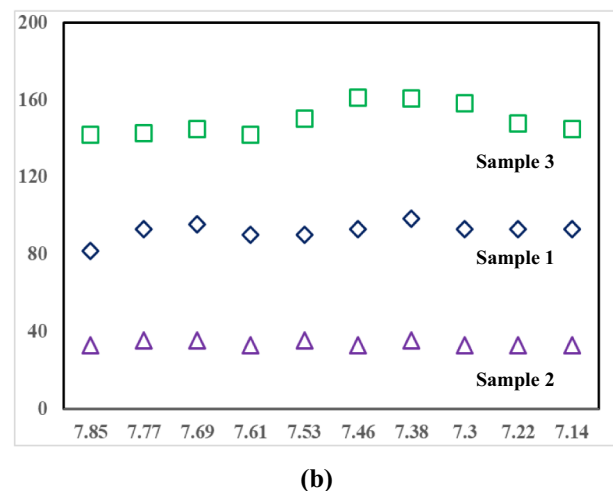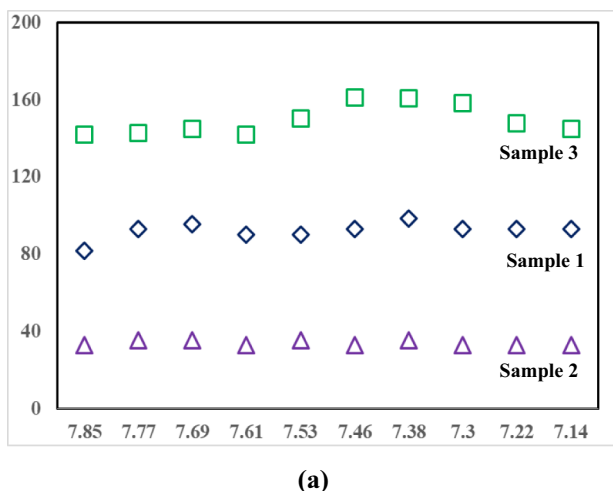
5 Variation in an aspect ratio

Experiments were performed to estimate the effects of an aspect ratio of the mixing channel, defined as h/w. The width of the mixing zone was measured perpendicular in the direction of flowing streams with increasing and decreasing flow rates at different aspect ratios in microchannel as shown in Fig. 5a, b, respectively.

When the aspect ratio tends towards low to high variations in the mixing zone decrease for a high aspect ratio due to a change in the non-uniform behaviour of diffusivity as suggested by Ismagilov et al. (2000). This non-uniform diffusion was characterized as the butterfly effect and the diffusive time scale had been varying between 0.35 and 0.5 across the channel depth by Kamholz and Yager (2001). The
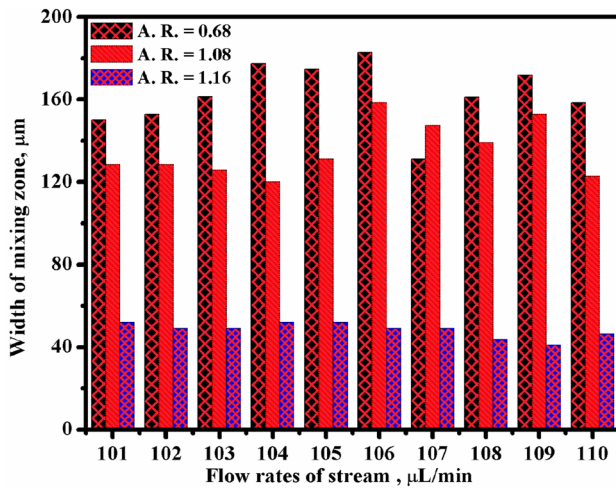
(a)
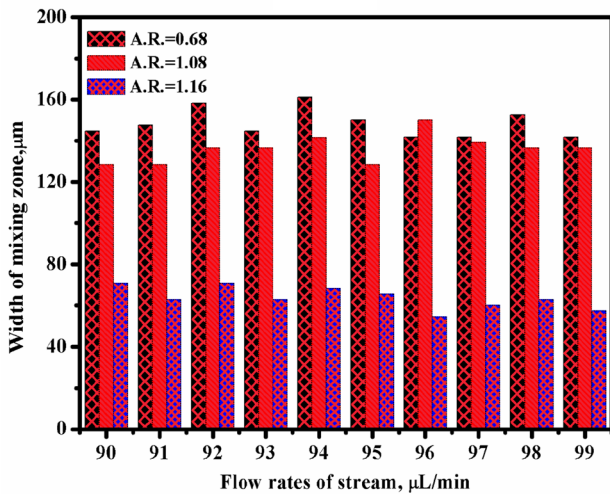
(b)

Fig. 5 Width of mixing zone related to inlet flow streams. **(a)** Increasing flow rates. **(b)** Decreasing flow rates

characteristics are also confirmed to vary with the aspect ratio with a change in the velocity profile. The non-uniform mixing shows to be more effective for the mixing channels with smaller aspect ratios. Besides this for channels with higher aspect ratios, where flow rate or velocity is chiefly characterized by the parabolic profile. It was established that the intensity of the mixing zone grows in a downstream direction based on the length scales. In the regime of non-uniform mixing, the channel depth is used as the length scale and the mixing intensity can be related to the different aspect ratios. As the mixing becomes uniform within the depth, its intensity is measured on the channel width to follow the

same rise as in the situation of uniform velocity (Chen et al. 2006).

6 Mixing performance

The mixing characteristics of T-shaped microchannels have been evaluated by Dreher et al. (2010) for all the regimes. They numerically established the degree of mixing as the mixing index (M.I.) on a certain cross-section of the mixing channel. The M.I. of the control area is based on the Danckwerts' intensity of segregation (Danckwerts 1952).

The mixing performance of the two co-flowing streams is based on the variance of the mass fraction from the mean concentration. The standard deviation of pixel intensity or point concentration is usually used as mixing performance or mixing index (M.I.) to evaluate mixing efficiency (Liu et al. 2000) and could be formulated as

$$\text{M.I.} = 1 - \sqrt{\frac{\sigma^2}{\sigma_{max}^2}} \tag{2}$$

$$\text{M.I.} = \sigma^2 = \frac{1}{N}\sum_{i=1}^{N}(c_i - \bar{c})^2 \tag{3}$$

An improved mixing index is also reported by (Tekin et al. 2011) and based on the comparison of standard deviation to the mean concentration or intensity and expressed as

$$\text{M.I.} = 1 - \frac{\sqrt{\frac{1}{N}\sum_{i=1}^{N}\left(c_i - \bar{c}\right)^2}}{\bar{c}} \tag{4}$$

To determine the mixing index from the equation, the extent of mixing in a specific cross-section of the channel, the ratio of the variance of the concentration (σ) and the maximum variance of concentration $\left(\sigma^2\right)$ can be selected here. N is the number of sample points on the plane perpendicular to the flow, c_i is the mass fraction value or point concentration or pixel intensity at the sampling point i on the cross-sectional of the channel, $\bar{c}$ is the average mixing value and it is taken 0.5 for average mixing.

The captured camera images were processed using Image J software recommended by the National Institute of Health, USA. The images were converted to grayscale images. These images were then analysed by constructing a perpendicular line across the channel to find out the change in the intensity across the channel. The change in the intensity of interdiffusion mixing of 20 initial images was analysed for each experiment. The formal fluctuations in the dye concentrations are caused by unstable flow fields, which might grow

during the analysis. The maximum variance at the inlet of the mixer is calculated by the formula.

$$\sigma^2_{max} = \sqrt{b(1-b)} \tag{5}$$

The higher the value of M.I., the larger the mixing efficiency. The mixing index range is from 0 to 1 (Wu et al. 2016). The zero value of M.I. represents unmixed conditions while 1 represents the complete mixed. Reynolds Number has an important dimensionless parameter that influences the fluid flow.

As the flow rates change there consequently varies in the mixing index. Increasing flow rates increases the mixing index and enhances the mixing effect because residence times changed. When it is increased 100–110 µl m^{-1} mixing process is higher because of fast fluid flow which

decreases the residence time inside the mixing channel, Fig. 6a. In addition, higher flow rates make convection partially dominant over diffusion which enhances the mixing index. Experiments showed that a higher mixing index was observed for the Acid red-water system due to its higher diffusion coefficient.
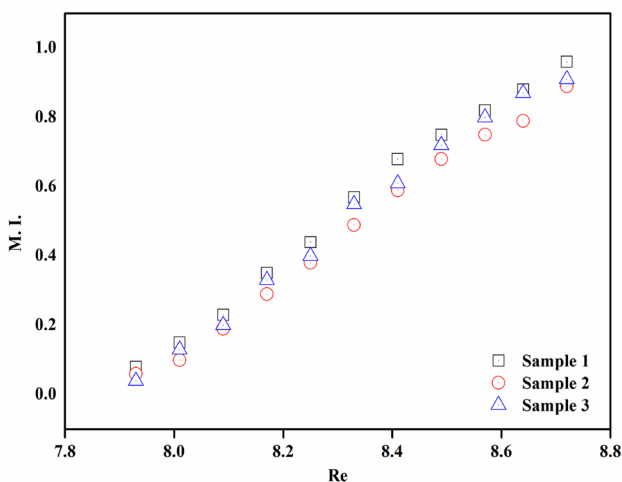
Decreasing flow rates, decrease the mixing index and the mixing process become slowly. Because of speed is low and the long residence time is seen in Fig. 6b. The residence time provides improves the diffusion process due to which mixing is taking place.

7 Analytical analysis of mixing in T-shaped microchannels

Let us consider the analysis of mixing phenomena between two miscible liquids in a T-shaped microchannel. It has two inlet channels and one mixing channel. The origin of coordinates is fixed at the point where the streams start to meet. As the streams move towards the mixing channel having rectangular cross-section height (h) × width (b) each liquid fill half of the cross-section. Since viscosities of both the liquids are the same and velocity profile is symmetric about the middle of the channel so that $x = 0$. Let us assume that the species concentration of liquid A is on the left half with the original concentration c_0 mixing with liquid B through convective and diffusive transport on the remaining right half as shown in Fig. 7. The fluid flow in the microfluidic channel is considered incompressible and under steady-state conditions, which is governed by the mass and momentum conservation equations (Bird et al. 2006).
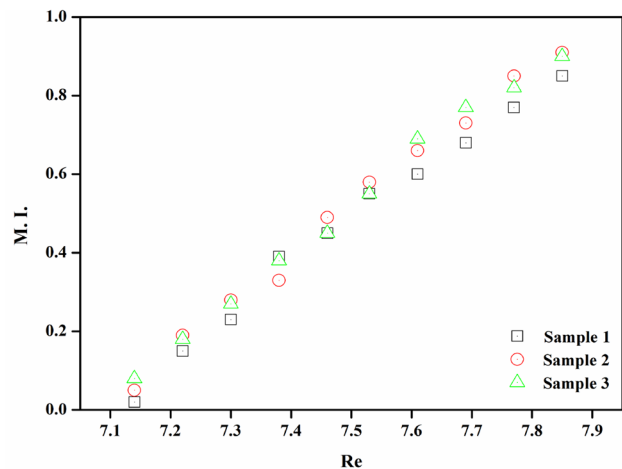
(a)

(b)

Fig. 6 Effect of flow rate on the mixing index. **(a)** Increasing flow rates. **(b)** Decreasing flow rates

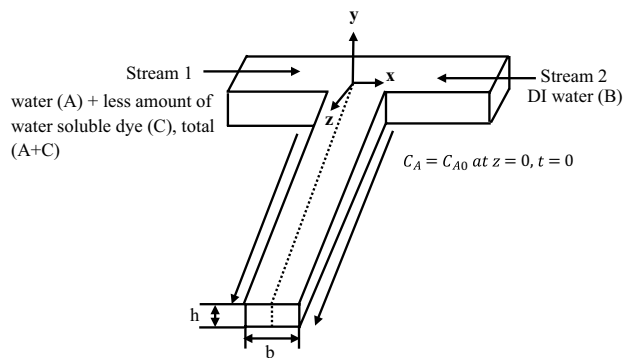**Fig. 7** Schematic of microchannel and coordinates for analytical analysis of mixing

$$Continuity: \frac{\partial V_x}{\partial x} + \frac{\partial V_y}{\partial y} + \frac{\partial V_z}{\partial z} = 0 \qquad (6)$$

Equation of continuity for species transport: convection and diffusion equation

$$\frac{\partial c}{\partial t} + u_x\frac{\partial C_A}{\partial x} + u_y\frac{\partial C_A}{\partial y} + u_z\frac{\partial C_A}{\partial z} = D\left[\frac{\partial^2 C_A}{\partial x^2} + \frac{\partial^2 C_A}{\partial y^2} + \frac{\partial^2 C_A}{\partial z^2}\right] + R$$

Rate of increase in moles A per unit volume	Net rate of addition of moles A per unit volume by convection	Rate of addition of moles A per unit volume by diffusion	Rate of production of moles A per unit volume by reaction

$$(7)$$

Here, c is the species concentration of liquid A, u_x, u_y and u_z components of velocity in the x, y and z directions, respectively. D is the diffusion coefficient. C_A is the change of concentration of liquid, R is the rate of production due to chemical reaction.

For this steady, non-reacting system there are no chemical reactions taking place so the rate of production term in Eq. (8) will be neglected. Further assumed that flow is fully developed and convection dominates over diffusion in the z-direction. The new form of Eq. (8) is given by

$$\left(\frac{\partial c}{\partial x}, y, z\right) = 0 \qquad (8)$$

where c stands for the mass concentration. To find out the mixing length required for the desired mixing in a T-shaped microchannel above analytical equation for convective-diffusive mass transport are solved using the method of separation of variables.

By neglecting the entrance region of the microchannel, it is assumed that the fluid flow is fully developed within the channel. It was also assumed that the velocity in Eq. (9) can be replaced by the average velocity of the channel.

Eq. (9) is called Fick's law of diffusion. This equation is generally used for diffusion in dilute liquid solutions at constant temperature and pressure.

Finally, the boundary conditions of this analysis can be specified as follows:

The above Eq. (3) is related to an initial condition of $c = 0$ at the channel entrance $z = 0$ and boundary conditions.

1. $C_A = C_{A0}$ at $z = 0$ and $C_A = 0$ at $z = \infty$.
2. $V = V_0$ at inlets, $V = 0$ at walls and $P = 0$ at the outlet

Also in consideration of zero-flux boundary conditions at the bottom, top and sidewalls,

$$\left(\frac{\partial c}{\partial x}, y, z\right) = 0 \qquad (9)$$

$$\left(\frac{\partial c}{\partial y}, \pm\frac{h}{2}, z\right) = 0 \qquad (10)$$

The species transport in 3-dimensional (3D)

On considering boundary conditions the Dirichlet boundary conditions $C = \frac{C_o}{2}$ and can be applied to the interface at the centre of the microchannel (Chen et al. 2006).

$$C = \frac{C_o}{2}, X = \frac{x}{b}, Y = \frac{y}{h}$$

From this dimensional formulation for Eq. (3) is

$$U_z\frac{\partial C}{\partial Z} = \frac{\partial^2 C}{\partial X^2} + \gamma^2\frac{\partial^2 C}{\partial X^2} \qquad (11)$$

For $0 > X < 1/2, -1/2 < Y < 1/2$
The initial and boundary conditions

$$C(0, Y, Z) = 1, \frac{\partial C}{\partial Z}(X, \pm1/2, Z) = \frac{\partial C}{\partial Y}(1/2, Y, Z)$$

$$= 0, C(X, Y, 0) = 0$$

where
$U_z = \frac{u_z}{u_0}$, is the normalised flow velocity
$\gamma = \frac{b}{h}$, is the aspect ratio

$$U_z = \frac{\pi}{4}\left[\sum_{k=1,3,5}^{\infty}\frac{1}{k^4}\left[\frac{\gamma}{2k\pi}\tanh\left(\frac{k\pi}{2\gamma}\right)\right]\right]-1 \qquad (12)$$

$$\sum_{k=1,3,5}^{\infty}\frac{(-1)^{\frac{k-1}{2}}}{k^3}\left[1-\frac{\cosh\left(\frac{k\pi Y}{\gamma}\right)}{\cosh\left(\frac{k\pi}{2\gamma}\right)}\right]\cos(k\pi X) \qquad (13)$$

The above equation represents that the velocity profiles of the flow and always shows a parabolic distribution across the Y-dimension on the centre of the channel ($X = 0$). In the case of a larger aspect ratio ($\gamma = 10$) and parabolic profile is given by

$$U_z = \frac{3}{2}\left(1-4Y^2\right) \qquad (14)$$

In the case of a smaller aspect ratio ($\gamma \sim 1$) the parabolic profile reduces slightly with the distance from the centre of the channel and leads to the no-slip boundary condition at the sidewalls.

Let us again consider, pressure-driven laminar flow of two adjacent streams in a single straight channel flowing in the z-direction. The interfacial region of a thickness δx, showing the thickness of molecular diffusion. The velocity profile is linear as away from the wall of the channel and given as $\delta_x \propto t^{1/2}$, further $\delta_x \propto z^{1/2}$ and near the wall velocity is linear as a function of distance along y-direction as shown in Fig. 7 also supported by Stone et al. (2004). Previously, Stone (1989), consider that the thickness δ_y of the diffusion boundary layer, this is due to molecular diffusion $\delta_y \propto Dt^{1/2}$. It represents that amount of sample reaches an axial location Z after covering the time z/G δ_y and $(G = \frac{\partial u_z}{\partial y})$. Thus finally, $\delta_y \propto (zD/t)^{1/3}$. Increasing in the thickness of concentration distribution in opposite direction or other transverse direction along x-direction also occurred only due to molecular diffusion and given by shear boundary layer as $\delta_y \propto \delta_x \propto (zD/t)^{1/3}$. It was also performed by Ismagilov et al. (2000) using confocal microscopy.

8 Conclusions

In conclusion, the influence of interdiffusion mixing zone for two miscible streams has been studied under various flow conditions, aspect ratios, and flowing streams. The efficient operation and precise control of process parameters at the microscale have facilitated by microfluidic devices (microchannels) that significantly improve the crystallization or nanoparticle synthesis process.

Two miscible streams (diluted dye and deionized water) flows parallel to each other under laminar flow conditions formed a dynamic or moving interface at the centre of the T-shaped microchannels. Under this situation, our aim is to maintain this moving interface in stable condition during the entire length of the channel to avoid stream crossover. The interdiffusion mixing width is measured vertically at this liquid–liquid interface when it becomes stable. Comparison in the interdiffusion mixing width observed and measured at constant and differential flow rates under low Reynolds number. Experiments confirmed that even at small changes in flow rates, geometries and diffusivities of flowing streams easily disturb the interface position corresponding to interdiffusion mixing width. Mixing performance and analytical evaluation of diffusion-dominated mixing were also reported in the current study. The paper provides information related to specific changes in crystallization or nanosynthesis such as crystal nucleation and growth, and nanocrystals. Analytical analysis of mixing was performed using convection–diffusion equation at a low Reynolds number and showed that the velocity profile become linear as it is away from the wall of the channel and it is a function of distance rather than time.

Controlled microfluidic interfaces can be used for various practical and industrial purposes like membraneless microfluidic fuel cells, drug delivery, protein crystallization, nanoparticle formation.

Declarations

Conflict of interest Author have no conflict of interest.

References

Agnihotri P, Lad VN (2018) Controlling interfacial mixing zone for microfluidic flow of liquid streams. J Braz Soc Mech Sci Eng 40:301. https://doi.org/10.1007/s40430-018-1203-8

Ansari MA, Kim K-Y, Kim SM (2018) Numerical and experimental study on mixing performances of simple and vortex micro T-mixers. Micromachines 9:204. https://doi.org/10.3390/mi9050204

Atencia J, Beebe DJ (2005) Controlled microfluidic interfaces. Nature 437:648–655. https://doi.org/10.1038/nature04163

Aubin J, Ferrando M, Jiricny V (2010) Current methods for characterising mixing and flow in microchannels. Chem Eng Sci 65:2065–2093. https://doi.org/10.1016/j.ces.2009.12.001

Bae JG, Park M, Kim DH, Lee YE, Kim Woo-Sik, Seo TS (2016) Tunable three-dimensional graphene assembly architectures through controlled diffusion of aqueous solution from a microdroplet. NPG Asia Mater 8:e329. https://doi.org/10.1038/am.2016.176

Bird RB, Stewart WE, Lightfoot EN (2006) Transport phenomena. Wiley, New York

Chen JM, Horng T-L, Tan WY (2006) Analysis and measurements of mixing in pressure-driven microchannel flow. Microfluid Nanofluid 2:455–469. https://doi.org/10.1007/s10404-006-0092-9

Cho HJ, Preston DJ, Zhu Y, Wang EN (2016) Nanoengineered materials for liquid–vapour phase-change heat transfer. Nat Rev Mater 2:16092. https://doi.org/10.1038/natrevmats.2016.92

Choban ER, Markoski LJ, Wieckowski A, Kenis PJA (2004) Microfluidic fuel cell based on laminar flow. J Power Sources 128:54–60. https://doi.org/10.1016/j.jpowsour.2003.11.052

Dambrine J, Geraud B, Salmon JB (2009) Interdiffusion of liquids of different viscosities in a microchannel. New J Phys 11:75015. https://doi.org/10.1088/1367-2630/11/7/075015

Danckwerts PV (1952) The definition and measurement of some characteristics of mixtures. Appl Sci Res Sect A 3:279–296. https://doi.org/10.1007/BF03184936

Demello AJ (2006) Control and detection of chemical reactions in microfluidic systems. Nature 442:394–402. https://doi.org/10.1038/nature05062

Dreher S, Engler M, Kockmann N, Woias P (2010) Theoretical and experimental investigations of convective micromixers and microreactors for chemical reactions. In: Bockhorn H, Mewes D, Peukert W, Warnecke HJ (eds) Micro and Macro Mixing. Heat and Mass Transfer. Springer, Berlin, Heidelberg. https://doi.org/10.1007/978-3-642-04549-3_18

Ferrigno R, Stroock AD, Clark TD, Mayer M, Whitesides MG (2002) Membraneless vanadium redox fuel cell using laminar flow. J Am Chem Soc 124:12930–12931. https://doi.org/10.1021/ja020812q

Gambhire S, Patel N, Gambhire G, Kale S (2016) A review on different micromixers and its micromixing within microchannel. Int J Curr Eng Technol 4:409–413. https://doi.org/10.13140/RG.2.1.4235.4324

Hatch A, Kamholz AE, Hawkins KR, Munson SM, Schilling AE, Weigl HB, Yager P (2001) A rapid diffusion immunoassay in a T-sensor. Nat Biotechnol 19:46. https://doi.org/10.1038/88135

Hatch A, Garcia E, Yager P (2004) Diffusion-based analysis of molecular interactions in microfluidic devices. Proc IEEE 92:126–139. https://doi.org/10.1109/JPROC.2003.820547

He M, Li W, Zhang M, Zhang J (2019) Numerical investigation on the efficient mixing of overbridged split-and-recombine micromixer at low Reynolds number. Microsyst Technol 25:3447–3461. https://doi.org/10.1007/s00542-019-04317-2

Hessel V, Löwe H, Schönfeld F (2005) Micromixers—a review on passive and active mixing principles. Chem Eng Sci 60:2479–2501. https://doi.org/10.1016/j.ces.2004.11.033

Hetsroni G, Mosyak A, Pogrebnyak E, Yarin LP (2005) Fluid flow in micro-channels. Int J Heat Mass Transf 48:1982–1998. https://doi.org/10.1016/j.ijheatmasstransfer.2004.12.019

Ismagilov RF, Stroock AD, Kenis PJA, Whitesides G (2000) Experimental and theoretical scaling laws for transverse diffusive broadening in two-phase laminar flows in microchannels. Appl Phys Lett 76:2376–2378. https://doi.org/10.1063/1.126351

Janasek D, Franzke J, Manz A (2006) Scaling and the design of miniaturized chemical-analysis systems. Nature 442:374. https://doi.org/10.1038/nature05059

Johnson TJ, Ross D, Locascio LE (2002) Rapid microfluidic mixing. Anal Chem 74:45–51. https://doi.org/10.1021/ac010895d

Kamholz AE, Yager P (2001) Theoretical analysis of molecular diffusion in pressure-driven laminar flow in microfluidic channels. Biophys J 80:155–160. https://doi.org/10.1016/S0006-3495(01)76003-1

Kamholz AE, Weigl BH, Finlayson BA, Yager P (1999) Quantitative analysis of molecular interaction in a microfluidic channel: the T-sensor. Anal Chem 71:5340–5347. https://doi.org/10.1021/ac990504j

Kamholz AE, Schilling EA, Yager P (2001) Optical measurement of transverse molecular diffusion in a microchannel. Biophys J 80:1967–1972. https://doi.org/10.1016/S0006-3495(01)76166-8

Kim D-J, Ha D, Zhou Q et al (2017) A cracking-assisted micro-/nanofluidic fabrication platform for silver nanobelt arrays and nanosensors. Nanoscale 9:9622–9630. https://doi.org/10.1039/C7NR02354E

Kumar V, Paraschivoiu M, Nigam KDP (2011) Single-phase fluid flow and mixing in microchannels. Chem Eng Sci 66:1329–1373. https://doi.org/10.1016/j.ces.2010.08.016

Li J, Barrow DA (2017) A new droplet-forming fluidic junction for the generation of highly compartmentalised capsules. Lab Chip 17:2873–2881. https://doi.org/10.1039/C7LC00618G

Liu RH, Stremler MA, Sharp KV et al (2000) Passive mixing in a three-dimensional serpentine microchannel. J Microelectromech Syst 9:190–197. https://doi.org/10.1109/84.846699

Ma J, Lee SM-Y, Yi C, Li C-W (2017) Controllable synthesis of functional nanoparticles by microfluidic platforms for biomedical applications—a review. Lab Chip 17:209–226. https://doi.org/10.1039/C6LC01049K

Mally M, Bozic B, Hartman SV et al (2017) Controlled shaping of lipid vesicles in a microfluidic diffusion chamber. RSC Adv 7:36506–36515. https://doi.org/10.1039/C7RA05584F

Marschewski J, Jung S, Ruch P et al (2015) Mixing with herringbone-inspired microstructures: overcoming the diffusion limit in co-laminar microfluidic devices. Lab Chip 15:1923–1933. https://doi.org/10.1039/C5LC00045A

Mousavi Shaegh SA, Nguyen N-T, Chan SH (2011) A review on membraneless laminar flow-based fuel cells. Int J Hydr Energy 36:5675–5694. https://doi.org/10.1016/j.ijhydene.2011.01.063

Nguyen N-T, Wu Z (2005) Micromixers—a review. J Micromech Microeng 15:R1. https://doi.org/10.1088/0960-1317/15/2/R01

Ottino JM, Wiggins S (2004) Introduction: mixing in microfluidics. Phil Trans R Soc Lond 362:923–935. https://doi.org/10.1098/rsta.2003.1355

Puigmartí-Luis J (2014) Microfluidic platforms: a mainstream technology for the preparation of crystals. Chem Soc Rev 43:2253–2271. https://doi.org/10.1039/c3cs60372e

Reckamp JM, Bindels A, Duffield S et al (2017) Mixing performance evaluation for commercially available micromixers using Villermaux–Dushman reaction scheme with the interaction by exchange with the mean model. Org Process Res Dev 21:816–820. https://doi.org/10.1021/acs.oprd.6b00332

Rismanian M, Saidi MS, Kashaninejad N (2019) A new non-dimensional parameter to obtain the minimum mixing length in tree-like concentration gradient generators. Chem Eng Sci 195:120–126. https://doi.org/10.1016/j.ces.2018.11.041

Sesen M, Alan T, Neild A (2017) Droplet control technologies for microfluidic high throughput screening (µHTS). Lab Chip 17:2372–2394. https://doi.org/10.1039/C7LC00005G

Shi H, Xiao Y, Ferguson S, Huang X, Wang N, Hao HX (2017) Progress of crystallization in microfluidic devices. Lab Chip 17:2167–2185. https://doi.org/10.1039/C6LC01225F

Squires TM, Quake SR (2005) Microfluidics: fluid physics at the nanoliter scale. Rev Mod Phys 77:977. https://doi.org/10.1103/RevModPhys.77.977

Stone HA (1989) Heat/mass transfer from surface films to shear flows at arbitrary Peclet numbers. Phys Fluids A 1:1112–1122. https://doi.org/10.1063/1.857335

Stone HA, Stroock AD, Ajdari A (2004) Engineering flows in small devices: microfluidics toward a lab-on-a-chip. Annu Rev Fluid Mech 36:381–411. https://doi.org/10.1146/annurev.fluid.36.050802.122124

Tan JN, Neild A (2012) Microfluidic mixing in a Y-junction open channel. AIP Adv 2:32160. https://doi.org/10.1063/1.4750483

Tekin HC, Sivagnanam V, Ciftlik AT et al (2011) Chaotic mixing using source–sink microfluidic flows in a PDMS chip. Microfluid Nanofluid 10:749–759. https://doi.org/10.1007/s10404-010-0706-0

Wang GR, Yang F, Zhao W (2014) There can be turbulence in microfluidics at low Reynolds number. Lab Chip 14:1452–1458. https://doi.org/10.1039/C3LC51403J

Wong SH, Ward MCL, Wharton CW (2004) Micro T-mixer as a rapid mixing micromixer. Sens Actuat B Chem 100:359–379. https://doi.org/10.1016/j.snb.2004.02.008

Wu C, Tang K, Gu B, Deng J, Liu Z, Wu Z (2016) Concentration-dependent viscous mixing in microfluidics: modelings and experiments. Microfluid Nanofluid 20:90. https://doi.org/10.1007/s10404-016-1755-9

Xia Y, Whitesides GM (1998) Soft lithography. Ann Rev Mater Sci 28:153–184. https://doi.org/10.1146/annurev.matsci.28.1.153

Zhao C-X, He L, Qiao SZ, Middelberg APJ (2011) Nanoparticle synthesis in microreactors. Chem Eng Sci 66:1463–1479. https://doi.org/10.1016/j.ces.2010.08.039